Gold Nano-Smolder for Biological Tissue Manipulation

F. Hajizadeh[a] and S. N. S. Reihani[b]

[a]Department of Physics, Institute for Advanced Studies in Basic Sciences, Zanjan, Iran
[b]Department of Physics, Sharif University of Technology, Tehran, Iran

Corresponding Authors: hajizade@iasbs.ac.ir, sreihani@physics.sharif.edu

ABSTRACT— Thanks to their unique optical and electromagnetic properties, noble-metal nanoparticles are proven very useful in many scientific fields, from nanotechnology to biology, including detection of cancer cells. Irradiated gold nanoparticles, as a nano-smolder could be widely used in biomedical contexts such as tumor therapy. Laser destruction of a cancerous tissue depends on thermal and physical properties of the tissue, therefore temperature quantification of an irradiated metallic nanoparticle in different materials could be followed by interesting applications. In this research we quantify the temperature of irradiated gold nanoparticles in paraffin which is the most commonly used material for embedding of biological tissues in pathology. We have shown that the temperature increase rate for irradiated gold nanoparticles with diameters of 78 nm, 97 nm, and 149 nm are 1.31, 1.40, and 2.28 °C/mW, respectively. Considering that the conductivity of a biological tissue is an important parameter on temperature raise and destruction, these results could yield a valuable insight into the cancer therapy.

KEYWORDS: Optical trapping, Photothermal effect, Gold nanoparticles, Nanotechnology, Biological and medical applications of laser.

I. INTRODUCTION

Noble metal nanoparticles with unique optical, thermal, and electromagnetic properties have become indispensable objects in molecular biology and medicine [1]. Metal, especially gold nanoparticles (GNPs), have the valuable advantage that their surface plasmon resonance may serve as an excellent real-time plasmonic detector of single molecules, without need for any labeling or amplification [2]. Optical trapping ability of GNPs has turned them to superior nanohandles for single-molecule force spectroscopy into the living cell in order to measure physical and biological properties at nano scale [3]. After first successful trapping of single GNP [4], during the last decade, there has been a considerable effort on broadening of the sizes range of the trappable GNPs [5,6] and today it is possible to trap single GNPs as small as 10 nm in diameter using a single beam Optical Tweezers (OT) [7]. Though temperature rise due to light absorption has been main concern for using GNPs in biological applications of OT, however, a hot GNP, as a "nano-smolder", could be a valuable tool for photo-thermal therapy of cancer [8].

Though there has been a great effort on measurement of heat produced by an irradiated GNP(s) in water-based samples [9-13], however, to our knowledge, there is no report on such characterization in non-aqueous media. In this paper we characterize the heat produced by an irradiated single GNP in paraffin wax. We have shown both by theory and experiment that a single GNP irradiated by few tens of milli-Watts of laser power could produce a nano-smolder as hot as 100 °C.

II. THEORY

Temperature distribution around an optically trapped single GNP using a laser beam with axial intensity profile of $I(z)$ and wavelength of λ can be described by heat transfer equation as (in absence of any phase transformation) [1]:

(1)

$$\rho(r)c(r)\frac{\partial T(r,t)}{\partial t}=\nabla k\nabla T(r,t)+Q(r,t) \quad (1)$$

where $T(r,t)$ defines the spatial and temporal variation of temperature. $\rho(r)$, $c(r)$ and $k(r)$ are mass density, specific heat, and thermal conductivity, respectively. $Q(r,t)$ denotes the local heat induced by absorption of the light by the single GNP.

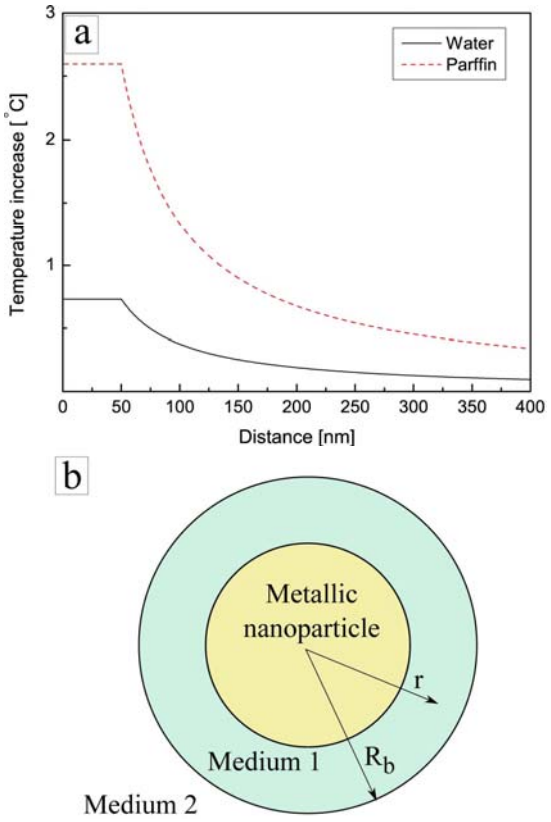

Fig. 1. (a) Calculated temperature increase around an optically trapped 100 nm GNP inside water (black solid line) and paraffin (red dashed line). P, ω_0, $k_0(water)$, and $k_0(paraffin)$ are considered to be 1 mW, 320 nm, 0.6 $W/m^{\circ}C$ and 0.2 $W/m^{\circ}C$ [14], respectively. (b) Schematic for two-phase medium around a hot metallic nanoparticle.

The steady state temperature profile in the surrounding medium can be deduced by solving Eq. (1) for $\frac{\partial T(r,t)}{\partial t}=0$:

$$\Delta T(r)=\frac{V_{np}Q}{4\pi k_0 r}=\frac{P_{abs}}{4\pi k_0 r}\ (r>R_{np}) \quad (2)$$

where k_0, r, V_{np}, and R_{np} are the thermal conductivity of surrounding medium, the radial distance from nanoparticle's center, the effective volume of the nanoparticle (the volume in which the electric filed is penetrated) [4], and the radius of nanoparticle, respectively. The absorption power, P_{abs}, is given by $P_{abs}=\sigma_{abs}I(z)$, in which the absorption cross section, σ_{abs}, for a Rayleigh particle subjected to a laser beam can be written as $\sigma_{abs}=2\pi n_m/\lambda\,\mathrm{Im}\left[3V_{np}\left(\varepsilon_{np}-\varepsilon_m\right)/\left(\varepsilon_{np}+2\varepsilon_m\right)\right]$ with ε_{np} and ε_m, respectively, representing the electric permittivity of the nanoparticle and surrounding medium and n_m being refractive index of the surrounding medium [4]. It should be mentioned that for a tightly focused TEM_{00} laser beam, the intensity profile along the optical axis can be written as $I(z)=P/[\pi\omega(z)^2]$ in which $\omega(z)=\omega_0\left[1+(z/z_0)^2\right]^{1/2}$ with P and $\omega(z)$ being the laser power and the beam diameter at a given axial position z, respectively [9]. It is worth mentioning that the smallest beam diameter ω_0 occurs at the focus, $z=0$. Fig. 1(a) shows the spatial profile of the temperature around a nanoparticle embedded into two different materials when illuminated using a focused laser. Note that due to the larger thermal conductivity of water (about three times larger than paraffin) the temperature drops more rapidly in water compare to the paraffin.

Consider the case where a spherical nanoparticle is positioned at the laser focus of an optical tweezers inside a medium such as paraffin. Temperature rise in the nanoparticle may cause phase transition or melting in the surrounding medium. To solve the heat transfer equations in such a system one has to consider three mediums as shown in Fig. 1(b). Temperature increase at position r inside the nanoparticle, medium 1, and medium 2, respectively, can be written as $\Delta T_{np}(r)=A-\frac{Q}{6k_{np}}r^2$ $\Delta T_1(r)=B+\frac{C}{r}$, $\Delta T_2(r)=\frac{D}{r}$, where A, B, C, and D are unknown coefficients [15]. From continuity boundary conditions for the temperature and energy flux at the interfaces,

the temperature increase inside the medium 1 can be written as [15]:

$$\Delta T_1(r) = \frac{P_{abs}}{4\pi R_b}\left(\frac{1}{k_2}-\frac{1}{k_1}\right)+\frac{P_{abs}}{4\pi k_2}\times\frac{1}{r}=\left(\alpha+\frac{\beta}{r}\right)P, \quad (3)$$

For a given laser power P, the radius of the boundary of mediums 1 and 2 can be given by:

$$R_b = \frac{\beta P}{\Delta T_1(R_b)-\alpha P}. \quad (4)$$

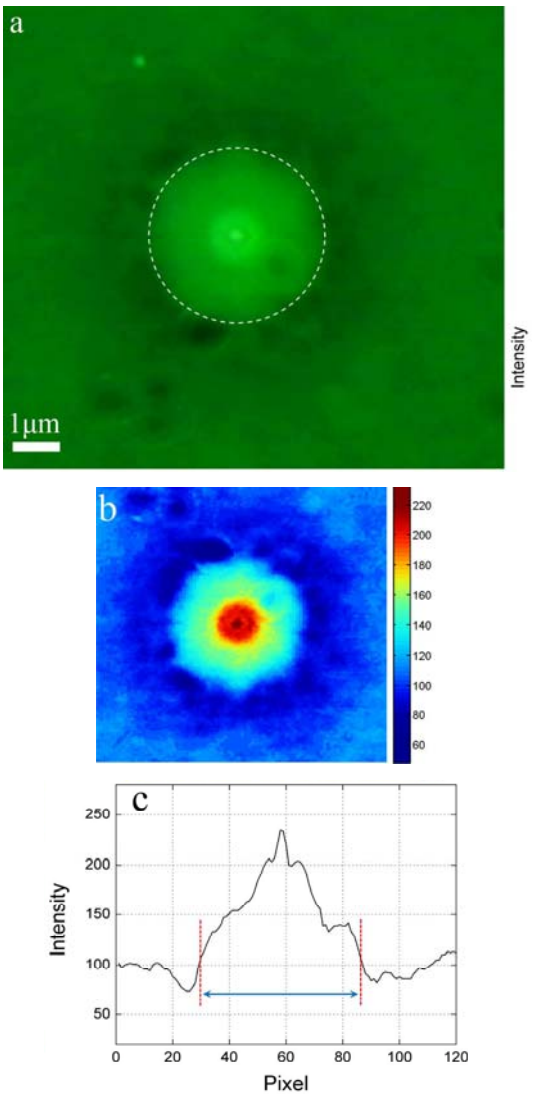

Fig. 2. (a) Phase contrast microscopy image of irradiated 97 nm GNP encapsulated in a few micrometer thick paraffin layer. Laser power at the sample was 60 mW, and the radius of circular border of the PTR (dashed circle) is 1.88 μm. (b) Three dimensional intensity profile around an irradiated nanoparticle. (c) Two dimensional data showing the intensity profile along a line around the irradiated nanoparticle.

III. EXPERIMENTS

First the GNPs were fixed on the surface of a cleaned coverglass as follows: Diluted GNP solution (300mM NaCl buffer) introduced into a chamber made of two cleaned coverglasses spaced by ~ 150 μm. The chamber was left for few hours to dry out. In order to make a thin layer of paraffin on top of the GNPs, first the chamber was opened up and few pieces of solid paraffin (Merck, product number 107157) was placed on top of the surface containing GNPs. The coverglass was places on top of a hot plate and heated up to 100°C so the paraffin was melted down. Later, a second cleaned coverglass was placed on top of the melted paraffin and pushed downward so that the thickness of the paraffin layer becames ~ 10 μm after which the chamber was cooled down. The GNPs with mean diameters of 78, 97, 149 nm used in this research were purchased from British Biocell (BBI). The standard deviation of the particle sizes was at most 10%, based on the company's report.

Our OT setup is based on a continuous wave laser beam (Nd:YAG, λ=1064 nm, Coherent) introduced into an inverted microscope (Olympus, IX-71). The laser beam is focused through a high numerical aperture objective lens (Olympus, 100×, NA=1.3, oil Ph3) to the diffraction limit. The sample chamber was mounted on a piezo stage (Physik Instrumente, PI-527.2cl) which along with a piezo equipped objective holder (Physik Instrumente, P-723.10) provides three dimensional positioning of the laser focus inside the sample chamber. The whole measurements were imaged using the phase contrast mode of the microscope to achieve better visibility. A temperature control system including a heater and circulator system (DAIHAN Scientific, WCH-8, temperature uniformity=0.2°) was used for changing the equilibrium temperature of the sample.

When a single GNP was positioned under the focus of the laser, the raise in temperature of the GNP eventually melted the paraffin in the vicinity of the GNP, such as a burning candle at the microscopic scale. Note that the

maximal heating occurs when the GNP is positioned exactly at the focus of the laser. In order to do so, the GNP was accurately positioned until the largest melted area occurred at a given laser power. Considering that in our case $\omega_0 = 320\,nm$ [16], nano-positioning ability was very crucial for this measurement.

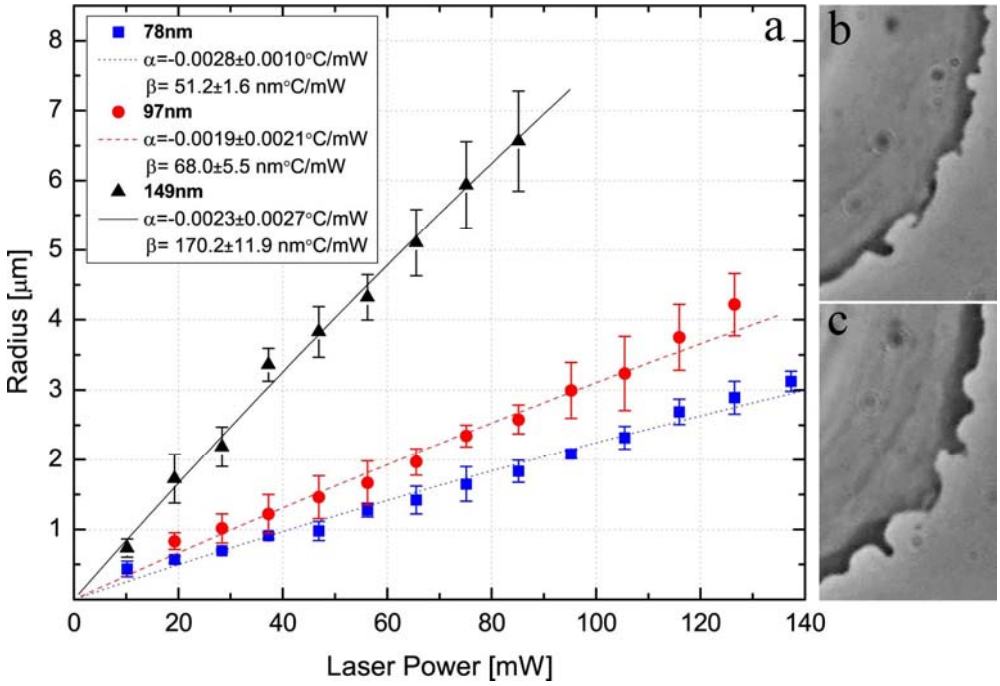

Fig. 3. The measured radius of phase transmitted region as a function of laser power at the sample. The lines show fit to Eq. (4). The right panel, (b) and (c), show the microscopy images from borders of a very thin layer of paraffin inside water at 25°C (a) and 27°C (phase transition temperature).

It is known that the paraffin waxes undergo a solid-solid phase transition at a specific temperature lower than melting temperature [17]. At this temperature a sudden drop in refractive index of the material occurs which facilitates visualization of this phase using the phase contrast microscopy technique. Figure 2(a) shows a typical phase contrast image of such an event in which the circular border of the Phase Transformed Region (PTR) could be easily recognized. A custom written MATLAB code was used to extract the average area (and radius) of PTR. Thereby, the radius of PTR could be extracted by three-dimensional (Fig. 2(b)) and two-dimensional (Fig. 2(c)) intensity profiling of the experimental image. The measurement was repeated with different laser powers for each GNP size and the results are summarized in Fig. 3. In order to convert the measured radii into the temperature, one has to know the temperature at which the solid-solid phase transition occurs for paraffin [17]. In order to measure this phase transition temperature (normally this temperature is not provided by the company), we performed an experiment as follows: First, a small piece of paraffin was melted on a cleaned coverglass surface using a hot plate after which, it was cooled down leaving a thin circular spot of paraffin on the coverglass. This coverglass was used to make a perfusion chamber using a second coverglass and two stripes of a double sided scotch tape. The chamber was filled with double-stilled water and placed on the microscope stage where the borders of the paraffin spot could be visualized. The equilibrium temperature of the chamber was increased very slowly with steps of 1°C while visualizing the borders of the paraffin spot. The right panel of Fig. 3 shows the border at 25°C (a) and 27°C (b).

Comparison of the images reveals that the rough edges in the upper image are rounded up in the lower image which could be a sign of the solid-solid phase transition. Therefore, during the main measurement, PTR radius (shown by a dashed circle in Fig. 2(a)) was assumed to be at 27°C.

It can be seen from Fig. 3 that: 1) The radius of PTR increases almost linearly with laser power (note that α is very small). 2) The radius grows more rapidly for larger GNPs which implies that the absorption cross section dramatically increases for larger GNPs. This could be of interest when the GNPs are to be used as nanoheaters. In order to extract the temperature on the nanoparticle, each experimental data set of Fig. 3 was fitted to Eq. (4) with $\Delta T_1(R_b) = 2^\circ C$ (the room temperature was 25°C). Finally by substituting the resulted values of α, β, and $r = R_{np}$ in Eq. (3) the temperature increase on the nanoparticle for each case was calculated. The final results were $1.31^\circ C/mW$ for 78 nm, $1.40^\circ C/mW$ for 97 nm, and $2.28^\circ C/mW$ for the 149 nm GNPs, respectively. Considering that the thermal conductivity of paraffin is three times smaller than that of the water, our experimental results are in agreement with previous reports of measurement in water [13]. The lower thermal conductivity of the paraffin could be of interest for the applications in which nanoparticles are to be used as nano-smolders.

To show that nanoparticles have the ability to destroy cancer cells, we perform an experiment in a pathology sample. In preparing of a pathology sample, paraffin is the most commonly used material for embedding of biological tissues. After the tissues have been dehydrated, cleared, and infiltrated with the embedding material, they are ready for external embedding. During this process the tissue samples are placed into molds along with liquid embedding material (paraffin wax) which is then hardened. This is achieved by cooling in the case of paraffin wax. Embedding provides support for tissue so that it is then ready to be sliced into very thin sections. Fig. 4 shows typical results of a biological manipulation in such a paraffin section.

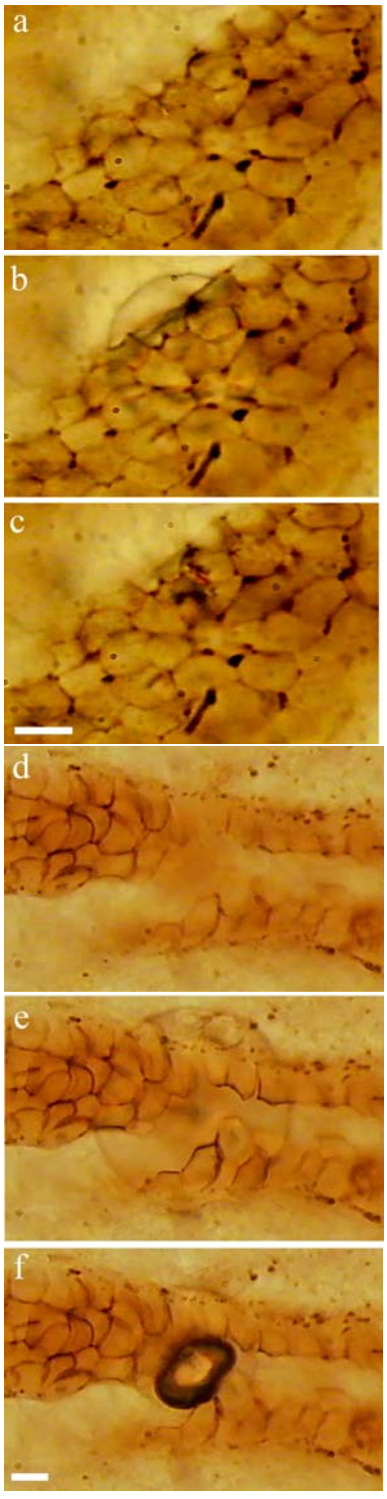

Fig. 4. Thermal micromanipulation of biological cells using gold nanoparticle irradiated by optical tweezers. Sample is a pathology tissue from human gallbladder embedded in paraffin. The a, c, and e (b, d, and f) panels show images taken using a $100\times(60\times)$ objective. The laser power at sample, respectively, were 0, 250, and 10 mW (0, 140, and 10 mW). The scale bars in both panels are 5 μm.

Thick tissue sections (~10 μm) are mounted on a cover glass where gold nanoparticles are stuck. In Fig. 4 a human gallbladder tissue embedded in paraffin is manipulated by use of a hot 78 nm (a, c, and e) and a 149 nm (b, d, and f) nano-smolder. The a and b images show the sample with zero laser power. The c-f images show the sample with a moderate laser power and after destruction, respectively. Note that the border of PTR can be recognized in the c and d images. The damage of the tissue in the position of the GNP is visible in the e and f images.

IV. CONCLUSION

We directly measured the heating rate associated with irradiated gold nanoparticles in paraffin. By measuring the phase change temperature for paraffin we could quantify the temperature on the surface of irradiated gold nanoparticles by use of the phase contrast microscopy. The heating rate for 78 nm, 97 nm, and 149 nm nanoparticles were measured to be 1.31, 1.40, and 2.28 $^{\circ}C/mW$, respectively. Considering that the thermal conductivity of paraffin is three times smaller than that of water, our experimental results are in agreement with previous reports of measurements in water. These results could be of great interest for biomedical community to use the local heat treatment of tissues as a complementary diagnostic and manipulation tool in pathology.

ACKNOWLEDGMENT

The authors acknowledge Ms. A. Tofighi for her technical discussion and valuable suggestions on pathology tissues. We are also grateful to Ms. B. Sharif for providing us with pathology samples.

REFERENCES

[1] A.O. Govorov and H.H. Richardon, "Generating heat with metal nanoparticles," Nano Today vol. 2, pp. 30–38, 2007.

[2] P. Zijlstra, P.M.R. Paulo, and M. Orrit, "Optical detection of single non-absorbing molecules using the surface plasmon resonance of a gold nanorod," Nature Nanotech, vol. 7, pp. 379–382, 2012.

[3] A. Veigel and C.F. Schmidt, "Moving into the cell: single-molecule studies of molecular motors in complex environments," Nature Rev. Mol. Cell Biol. Vol. 12, pp. 163–176, 2011.

[4] K. Svoboda and S.M. Block, "Optical trapping of metallic Rayleigh particles," Opt. Lett. Vol. 19, pp. 930–932, 1994.

[5] P.M. Hansen, V.K. Bhatia, N. Harrit, and L.B. Oddershede, "Expanding the optical trapping range of gold nanoparticles," Nano Lett. Vol. 5, pp. 1937–1942, 2005.

[6] K. Pearce, F. Wang, and P.J. Reece, "Dark-field optical tweezers for nanometrology of metallic nanoparticles," Opt. Express, vol. 19, pp. 25559–15569, 2011.

[7] F. Hajizadeh and S.N.S. Reihani, "Optimized optical trapping of gold nanoparticles," Opt. Express, vol. 18, pp. 551–559, 2010.

[8] P.K. Jain, I.H. El-Sayeda, and M.A. El-Sayed, "Au nanoparticles target cancer," Nano Today vol. 2, pp. 18–29, 2007.

[9] Y. Seol, A.E. Carpenter, and T.T. Perkins, "Gold nanoparticles: enhanced optical trapping and sensitivity coupled with significant heating, " Opt. Lett. Vol. 31, pp. 2429–2431, 2006.

[10] H.H. Richardson, Z.N. Hickman, A.O. Govorov, A.C. Thomas, W. Zhang, and M.E. Kordesch, "Thermooptical properties of gold nanoparticles embedded in ice: characterization of heat generation and melting," Nano. Lett. Vol. 6, pp. 783–788 2006.

[11] J. Shah, S. Park, S. Aglyamov, T. Larson, L. Ma, K. Sokolov, K. Johnston, T. Milner, and S.Y. Emelianov, "Photoacoustic imaging and temperature measurement for photothermal cancer therapy," J. Biomed. Opt. vol. 13, pp. 034024 (1–9), 2008.

[12] M. Honda, Y. Saito, N.I. Smith, K. Fujita, and S. Kawata, "Nanoscale heating of laser irradiated single gold nanoparticles in liquid," Opt. Express, vol. 19, pp. 12375–12383, 2011.

[13] P.M. Bendix, S.N.S. Reihani, and L.B. Oddershede, "Direct measurements of heating by electromagnetically trapped gold nanoparticles on supported lipid bilayers," ACS Nano, vol. 4, pp. 2256–2262, 2010.

[14] M.M. Farid, A.M. Khudhair, S.A.K. Razack, and S. Al-Hallaj, "A review on phase change energy storage: materials and applications," Energy Convers. Manage. Vol. 45, pp. 1597–1615, 2004.

[15] A.O. Govorov, W. Zhang, T. Skeini, H. Richardson, J. Lee, and N.A. Kotov, "Gold nanoparticle ensembles as heaters and actuators: melting and collective plasmon resonances," Nanoscale Res. Lett. Vol. 1, pp. 84–90, 2006.

[16] A. Pralle, M. Prummer, E. -L. Florin, E. H. K. Stelzer, and J. K. H. Hörber, "Three-dimensional high-resolution particle tracking for optical tweezers by forward scattered light," Microsc. Res. Tech. Vol. 44, pp. 378–386, 1999.

[17] J.F. Johnson, "Phase transformations in commercial paraffin waxes," Ind. Eng. Chem. Vol. 46, pp. 1046–1048, 1954.

Faegheh Hajizadeh was a student of the continuous track PhD Program at Institute for Advanced Studies in Basic Sciences (IASBS) Zanjan, Iran. She obtained her Ph.D. degree in Physics-Optics from IASBS in Oct. 2011. The main scientific objective of her PhD research was the optical trapping of gold nanoparticles in optimized conditions, under the supervision of Dr. S. Nader S. Reihani.

Seyed-Nader Seyed-Reihani received his BSc degree in Physics from Tabriz University, Tabriz, Iran in 1993, MSc degree in Physics from Sharif University of Technology, Tehran, Iran in 1996, and PhD degree in Physics from Institute for Advanced Studies in Basic Sciences (IASBS), Zanjan, Iran in 2005.

From 2005 to 2007 he was a Post-Doc fellow at the Niels Bohr Institute (NBI), Copenhagen University, Copenhagen, Denmark. From 2007 to 2013 he was an assistant professor in the department of Physics at IASBS. In 2013 he joined Sharif University where he is currently an assistant professor. His research interests include physical optics, optical trapping of nanoparticles, micromanipulation of biological tissues by use of Optical Tweezers.

Dr. Seyed-Reihani is a member of Optical Society of America (OSA) and Optics and Photonics Society of Iran (OPSI).

THIS PAGE IS INTENTIONALLY LEFT BLANK.